Knockdown of ASF1B inhibits cell proliferation, migration, invasion and cisplatin resistance in gastric cancer through the Myc pathway

ZAO ZHANG, MEIYING NING, LI LI, ZHUANGZHUANG LI, YANRONG WANG and JING ZHAO

Department of Pharmacy, Cangzhou Central Hospital, Cangzhou, Hebei 061000, P.R. China

Received November 30, 2022; Accepted March 7, 2023

DOI: 10.3892/ol.2023.13828

Abstract. Gastric cancer (GC) is a prevalent malignancy in the digestive system that poses a serious threat to human health. Anti-silencing function 1B (ASF1B) performs an important role in the progression of numerous tumors; however, its function in GC still requires further elucidation. Using data from The Cancer Genome Atlas, the expression levels of ASF1B in GC tissues were analyzed and a survival curve for high-ASF1B expression and low-ASF1B expression groups was plotted using the Kaplan-Meier method. Reverse transcription-quantitative PCR was performed to evaluate ASF1B expression in GC tissues and cells. Small interfering RNAs targeting ASF1B were transfected into HGC-27 and AGS cells to silence ASF1B expression. Cell viability, proliferation, migration, invasion, and apoptosis in HGC-27 and AGS cells was assessed using cell counting kit-8 assay, colony formation assay, wound healing assay, Transwell assay and flow cytometry, respectively. The protein changes were assessed using western blotting. Gene Set Enrichment Analysis (GSEA) was used to identify ASF1B related pathways. The results demonstrated that ASF1B expression was increased in GC tissues and cells compared with adjacent healthy tissues and normal cells (GES-1), and high expression of ASF1B was associated with poor survival outcomes in patients with GC. Silencing ASF1B inhibited cell viability, colony formation, migration, invasion and cisplatin resistance, while also attenuating the apoptotic capability of HGC-27 and AGS cells. GSEA showed that ASF1B could activate the Myc-targets-v1 and Myc-targets-v2 pathways. Moreover, silencing ASF1B inhibited the Myc pathway-related proteins Myc, minichromosome maintenance (MCM)4 and MCM5. Overexpression of Myc reversed the inhibitory effect of ASF1B silencing on AGS cell proliferation, invasion and cisplatin resistance. In conclusion, the results indicate that knockdown of ASF1B may suppress GC cell proliferation, migration and invasion, and promote cell apoptosis and cisplatin sensitivity by modulating the Myc pathway, thereby offering novel possibilities for reversing cisplatin resistance in GC.

Correspondence to: Dr Zao Zhang, Department of Pharmacy, Cangzhou Central Hospital, 50 Xinhua Middle Road, Cangzhou, Hebei 061000, P.R. China
E-mail: aogg8202@163.com

Abbreviations: ASF1B, anti-silencing function 1B; GC, gastric cancer

Key words: gastric cancer, ASF1B, cisplatin resistance, Myc pathway

Introduction

Gastric cancer (GC) is a major unresolved digestive problem that affects >1 million patients worldwide (1,2). Due to the increasing incidence rate (5.6%) and mortality rate (7.7%), GC is now considered the fifth most common and fourth most lethal tumor worldwide (3). While the 5-year survival rate for early GC is >90%, most patients present with advanced-stage GC due to the low early diagnosis rate (4). Treatment strategies for GC are rapidly evolving, and systemic chemotherapy, immunotherapy, radiotherapy and targeted therapy have all been effective in curing the tumor. Among them, surgery is the most efficient, but the recurrence rate for patients with GC is high (5). A previous study reported that patients with GC who undergo surgery have a poor 5-year survival rate of 60-80% (1). These findings highlight the importance of developing efficacious targeted therapies (1).

Cisplatin is widely used to treat various types of solid cancers, including ovarian, non-small-cell lung, breast and muscle-invasive bladder cancer (6-9). Studies have revealed that cisplatin plays an anticancer role through a number of mechanisms. The most widely accepted mechanism is that cisplatin inhibits the synthesis of DNA, mRNA and proteins, thereby leading to cell death (10-12). However, the major challenges associated with cisplatin are resistance and toxicity (13). Therefore, deciphering the effect of cisplatin response is helpful in identifying novel potential targets for combinatory therapies in cancer.

Anti-silencing function 1 (ASF1), an important chaperone protein of histones H3/H4, performs an important role in DNA replication, damage response and transcription (14). ASF1 has two paralogs, ASF1A and ASF1B. Previous studies have suggested that ASF1A is primarily involved in DNA repair and cell senescence, whereas ASF1B is associated with cell proliferation (15,16). Other studies have shown that dysregulation of ASF1B expression is linked to the progression and

metastasis of multiple cancers, including cervical cancer, thyroid cancer, hepatocellular carcinoma and clear cell renal cell carcinoma (15,17-19). However, the functional role of ASF1B in GC requires further investigation.

In the present study, the aim was to evaluate the function and possible mechanisms of ASF1B in GC. Here, we constructed ASF1B knockdown cells and detected the biological behavior changes using colony formation, wound healing and Transwell assays, and flow cytometry. The present study may provide a therapeutic strategy for patients with GC experiencing cisplatin resistance.

Materials and methods

Bioinformatics analysis. The RNA-sequencing expression profiles and clinical data were obtained from The Cancer Genome Atlas-Stomach Adenocarcinoma (TCGA-STAD) database (https://portal.gdc.cancer.gov) to examine the expression of ASF1B. The Kaplan-Meier Plotter online database (https://kmplot.com/analysis/index.php?p=service&cancer=gastric) was used for the Kaplan-Meier analysis (20). The Kaplan-Meier method followed by the log-rank test was employed to plot and analyze the survival curves of STAD patients with high/low expression of ASF1B. According to the autoselected best cutoff value of 285, patients were divided into two groups (high and low) for the survival analysis. The underlying mechanism of ASF1B in GC and pathway enriched genes were explored using Gene Set Enrichment Analysis (GSEA) based on the clinical data of TCGA database (21). GSEA parameter settings were as follows: Number of permutations=1000, permutation type=gene_set, enrichment statistic=weighted, metric for ranking genes=Signal2Noise. Venny 2.1 (https://bioinfogp.cnb.csic.es/tools/venny/) was used to highlight the intersecting genes. Pearson's correlation analysis was used to explore the correlation between the expression of the ASF1B gene and that of other key genes, such as Myc, minichromosome maintenance (MCM)4 and MCM5.

Tissue samples from patients with GC. A total of 25 pairs of GC and adjacent healthy tissues (>5 cm from the tumor tissues) from patients with GC (age, 26-73 years; female, 9; male, 16) were acquired between July 2021 and June 2022, and tissues were immediately frozen in liquid nitrogen and stored at -80˚C. The inclusion criteria were as follows: i) Patients were diagnosed with GC by pathology; ii) before surgery, patients didn't receive any treatment, such as chemotherapy and/or radiotherapy. The exclusion criteria were as follows: i) Patients had other malignant tumors or critical illness, such as coronary heart disease or diabetes; ii) patients didn't sign informed consent for the use of their tissues. All samples were obtained from Cangzhou Central Hospital (Cangzhou, China) in accordance with the ethical and legal standards of the Ethics Committee of Cangzhou Central Hospital (approval no. 2021-018-01).

Cell culture. The human gastric epithelial cell line GES-1 and the GC cell lines HGC-27 and AGS were purchased from The Cell Bank of Type Culture Collection of The Chinese Academy of Sciences. All cells were maintained in DMEM (Gibco; Thermo Fisher Scientific, Inc.) containing 10% FBS (Gibco; Thermo Fisher Scientific, Inc.) and 1% penicillin-streptomycin solution (Gibco; Thermo Fisher Scientific, Inc.) in a humidified atmosphere at 37˚C and 5% CO_2.

Cell transfection and treatment. Small interfering (si)RNAs against ASF1B and scrambled siRNA negative control (si-NC) were obtained from Shanghai GenePharma Co. Ltd. as follows: si1-ASF1B sense, 5'-GUUGUGAUUGCUGUUUGUAUA-3' and antisense, 5'-UACAAACAGCAAUCACAACAG-3'; si2-ASF1B sense, 5'-UGUGGAUGCUGUUGUGAUUGC-3' and antisense, 5'-AAUCACAACAGCAUCCACAUG-3'; and si-NC sense, 5'-UUCUCCGAACGUGUCACGUTT-3' and antisense, 5'-ACGUGACACGUUCGGAGAATT-3'. The Myc gene was cloned into the pcDNA3.1 vector (Guangzhou RiboBio Co., Ltd.) to overexpress Myc. The pcDNA3.1 empty vector (Guangzhou RiboBio Co., Ltd.) was employed as NC. HGC-27 and AGS cells were divided into the following groups: i) si-NC (cells were transfected with 50 nM si-NC for 48 h at 37˚C); ii) si1-ASF1B (cells were transfected with 50 nM si1-ASF1B for 48 h at 37˚C); iii) si2-ASF1B (cells were transfected with 50 nM si2-ASF1B for 48 h at 37˚C); iv) si-NC + cisplatin (HGC-27 cells were transfected with 50 nM si-NC for 48 h at 37˚C and then treated with 6.8 μM cisplatin for 48 h at 37˚C; AGS cells were transfected with 50 nM si-NC for 48 h at 37˚C and then treated with 13.3 μM cisplatin for 48 h at 37˚C); and v) si2-ASF1B + cisplatin (HGC-27 cells were transfected with 50 nM si2-ASF1B for 48 h at 37˚C and then treated with 6.8 μM cisplatin for 48 h at 37˚C; AGS cells were transfected with 50 nM si2-ASF1B for 48 h at 37˚C and then treated with 13.3 μM cisplatin for 48 h at 37˚C). Additionally, AGS cells were also divided into the following groups: i) Vector (cells were transfected with 2 μg pcDNA3.1 empty vector for 48 h at 37˚C); ii) Myc (cells were transfected with 2 μg pcDNA3.1-Myc for 48 h at 37˚C); iii) si2-ASF1B + Vector (cells were transfected with 50 nM si2-ASF1B and 2 μg pcDNA3.1 empty vector for 48 h at 37˚C); iv) si2-ASF1B + Myc (cells were transfected with 50 nM si2-ASF1B and 2 μg pcDNA3.1-Myc for 48 h at 37˚C); v) si2-ASF1B + Vector + cisplatin (cells were transfected with 50 nM si2-ASF1B and 2 μg pcDNA3.1 empty vector for 48 h at 37˚C and then treated with 13.3 μM cisplatin for 48 h at 37˚C); and vi) si2-ASF1B + Myc + cisplatin (cells were transfected with 50 nM si2-ASF1B and 2 μg pcDNA3.1-Myc for 48 h at 37˚C and then treated with 13.3 μM cisplatin for 48 h at 37˚C). Cisplatin was purchased from MedChemExpress. Lipofectamine® 3000 (Invitrogen; Thermo Fisher Scientific, Inc.) was used for transfection. After transfection for 48 h, cells were harvested for subsequent experiments.

RNA extraction and reverse transcription-quantitative PCR (RT-qPCR). TRIzol® (Invitrogen; Thermo Fisher Scientific, Inc.) reagent was used to isolate total RNA from GC cells and tissues. Complementary DNA was prepared using PrimeScript™ RT Reagent Kit (Takara Bio, Inc.) according to the manufacturer's protocol. Subsequently, RT-qPCR was performed using SYBR Premix Ex Taq II (Takara Bio, Inc.) and the 7900HT PCR system. The following thermocycling conditions were used: Initial denaturation at 95˚C for 1 min, followed by 39 cycles of 95˚C for 30 sec, 60˚C for 30 sec and

72˚C for 30 sec. The mRNA expression of Myc and ASF1B was normalized to that of the reference gene, GAPDH, and quantified using the $2^{-\Delta\Delta Cq}$ method (22). All primers used were purchased from Shanghai GenePharma Co. Ltd. The primer sequences were as follows: ASF1B forward, 5'-ATGTTT GTCTTTCAGGCCGAC-3' and reverse, 5'-GCTCAGGGT TGAGGTACTCG-3'; Myc forward, 5'-TGGAAAACCAGC CTCCCGC-3' and reverse, 5'-CGAAGGGAGAAGGGTGTG AC-3'); and GAPDH forward, 5'-GTTGCAACCGGGAAG GAAAT-3' and reverse, 5'-GCCCAATACGACCAAATC AGA-3'.

Western blotting. HGC-27 and AGS cells were lysed using RIPA buffer (MilliporeSigma) containing 1% protease inhibitors. Total protein was quantified using a BCA assay and 30 μg protein/lane was separated by SDS-PAGE on 12% gels. The separated proteins were subsequently transferred onto PVDF membranes. After blocking with 5% non-fat dry milk for 1 h at 37˚C, the membranes were incubated with primary antibodies against ASF1B (1:1,000, cat. no. 2902, Cell Signaling Technology, Inc.), MMP-7 (1:1,000, cat. no. 3801, Cell Signaling Technology, Inc.), MMP-9 (1:1,000, cat. no. ab76003, Abcam), anti-Myc (1:1,000, cat. no. SAB4501941, Sigma-Aldrich), MCM4 (1:1,000, cat. no. 12973, Cell Signaling Technology, Inc.), MCM5 (1:1,000, cat. no. ab75975, Abcam) and GAPDH (1:1,000, cat. no. ab9485, Abcam) at 4˚C overnight. Membranes were washed three times with PBS with 0.5% Tween 20. Following the primary incubation, membranes were incubated with HRP-conjugated goat anti-rabbit IgG secondary antibodies (1:5,000, cat. no. ab97051, Abcam) for 2 h at room temperature. Protein bands were visualized using enhanced chemiluminescence detection kit (MilliporeSigma), and semi-quantified using ImageJ v1.8.0 software (National Institutes of Health) with GAPDH as the loading control.

Cell viability assay. HGC-27 and AGS cells in the logarithmic growth phase were maintained in 96-well plates with a density of 1,000 cells/well. Following incubation for 0, 24, 48 and 72 h at 37˚C, 10 μl Cell Counting Kit-8 (CCK-8) reagent (Beyotime Institute of Biotechnology) was placed into each well and cells were incubated for another 1.5 h. The absorbance at 450 nm was examined using a microplate reader (Tecan Group, Ltd.).

Colony formation assay. During the logarithmic growth phase, HGC-27 and AGS cells were harvested to examine their clonogenic capability. The cells ($1x10^3$ cells per well) were inoculated into 30-mm dishes with DMEM +10% FBS and cultured at 37˚C for 14 days. The culture medium was refreshed every 2 days. The cells were subsequently fixed in 4% paraformaldehyde for 30 min at room temperature, and stained using 0.1% crystal violet for 20 min at room temperature. Finally, the number of colonies with >50 cells was calculated with blinded manual counting.

Wound healing assay. HGC-27 and AGS cells ($2x10^6$ cells/well) were plated into 6-well plates and cultured in serum-free medium. A 200 μl sterile pipette tip was used to scratch the cell monolayer when cell confluence was >90%. All detached cells were removed with PBS and the remaining cells were imaged at 0 and 48 h under a light microscope (Olympus Corporation). The wound area was determined using ImageJ v1.8.0 software (National Institutes of Health) according to the following formula: Wound healing rate (%)=$(A_0-A_t)/A_0$, where A_0 indicates the initial wound area and A_t indicates the wound area after 48 h.

Transwell assay. Cell invasive ability was detected using 24-well Transwell chambers (0.8 μm; Corning, Inc.). Transwell chambers were pre-coated with Matrigel (BD Biosciences) for 45 min at 37˚C HGC-27 and AGS cells at a density of $2x10^4$ in 100 μl DMEM were plated into the upper chambers. A total of 500 μl DMEM including 10% FBS were used to fill the lower chamber. After incubation for 48 h at 37˚C, the non-invaded cells were removed using swabs, while the remaining cells were fixed in 100% methanol for 10 min at room temperature and stained using 0.1% crystal violet for 20 min at room temperature. All cells were washed with PBS twice and counted from five randomly selected fields of view. Images were captured using a light microscope.

Apoptosis analysis. Annexin V-FITC Apoptosis Detection Kit (Beyotime Institute of Biotechnology) was applied to detect HGC-27 and AGS cell apoptosis. Briefly, cells were collected in 5 ml tubes and centrifuged at 1,000 x g for 5 min at 4˚C. Pre-chilled PBS was used to resuspend cells prior to being centrifuged as aforementioned. After the supernatant had been removed, 1X binding buffer was used to resuspend cells at a density of $1x10^6$ cells/ml. Cells were stained with 5 μl Annexin V-FITC in the dark for 5 min at room temperature, followed by incubation with 10 μl PI for 15 min at room temperature. Apoptotic cells were subsequently analyzed using a BD Accuri C6 flow cytometer (BD Biosciences). Cell apoptosis rate (upper right + lower right) were analyzed by FlowJo V7.6 software (FlowJo LLC).

Statistical analysis. For each assay, 3 independent repeats were performed. Data were analyzed using GraphPad Prism (version 8.0; Dotmatics). All data are presented as the mean ± standard deviation. The comparison between two groups was analyzed using Student's t-test (paired or unpaired), while differences between multiple groups were analyzed using one-way ANOVA followed by Tukey's post-hoc test. $P<0.05$ was considered to indicate a statistically significant difference.

Results

ASF1B expression is increased in GC tissues and cells and is associated with an unfavorable outcome in patients with GC. Analysis of data from TCGA database showed that ASF1B exhibited higher expression in GC tissues compared with normal tissues (Fig. 1A). Survival curve analysis showed that high ASF1B expression was indicative of a poor prognosis in patients with GC (Fig. 1B). RT-qPCR was performed to examine the expression of ASF1B in tumor and healthy tissues, indicating that ASF1B expression was increased in GC compared with adjacent healthy tissues (Fig. 1C). Moreover, compared with GES-1 cells, ASF1B expression was elevated both in HGC-27 and AGS GC cell lines (Fig. 1D).

Silencing of ASF1B suppresses proliferation and increases apoptosis in GC cells. To explore the role of ASF1B, HGC-27

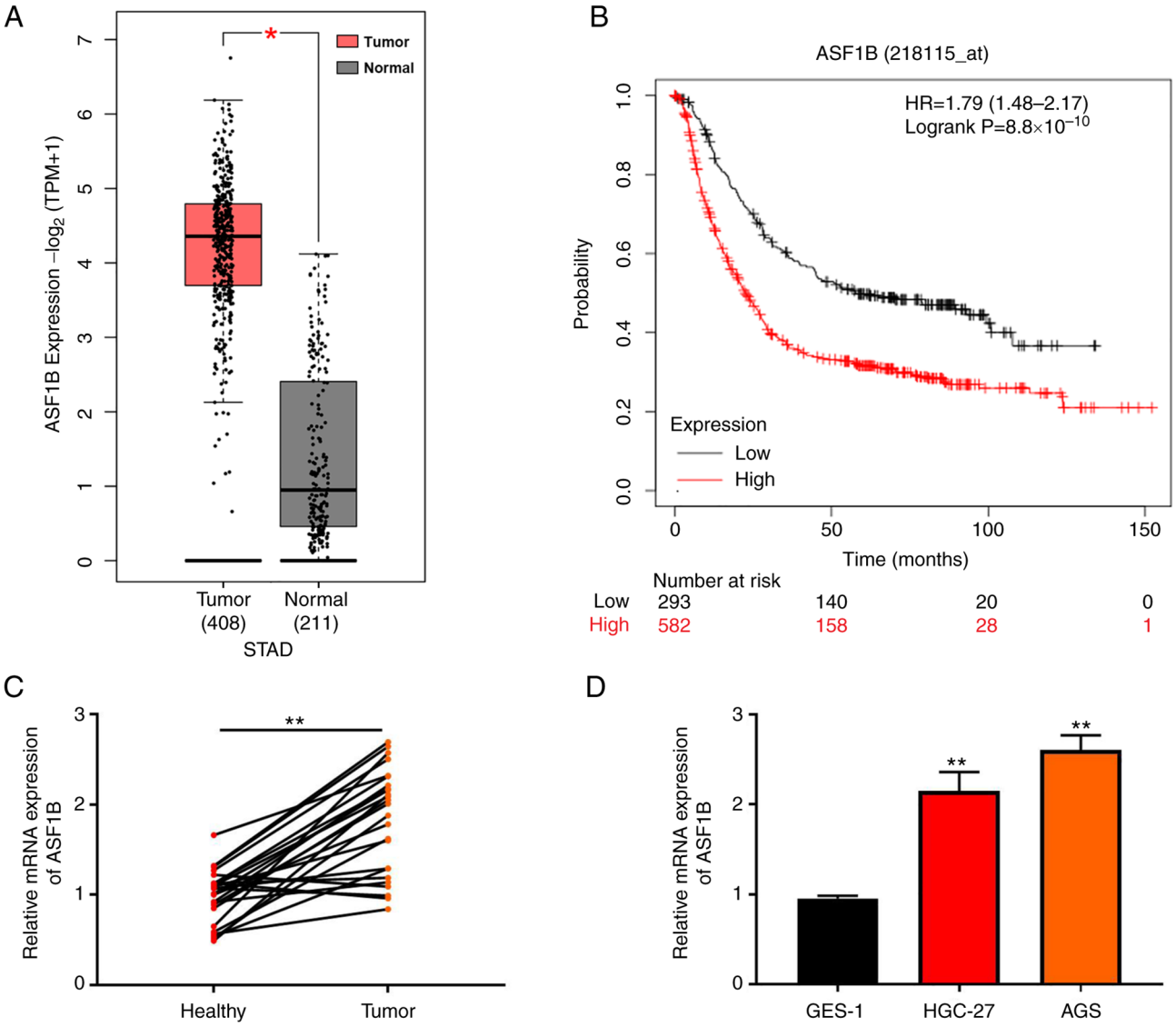

Figure 1. ASF1B is highly expressed in GC tissues and cells. (A) TCGA database analysis showed that ASF1B expression was increased in GC tissues compared with healthy tissues. (B) Survival analysis was performed using the Kaplan-Meier method based on data from TCGA database. (C) RT-qPCR analysis was implemented to evaluate the expression level of ASF1B in GC tissues and adjacent healthy tissues of 25 patients with GC. (D) ASF1B mRNA expression in GES-1 cells and HGC-27 and AGS GC cells was measured using RT-qPCR. *P<0.05 and **P<0.01 compared with GES-1 or as indicated. GC, gastric cancer; TCGA, The Cancer Genome Atlas; RT-qPCR, reverse transcription-quantitative PCR; ASF1B, anti-silencing function-1B; TPM, transcripts per million; STAD, stomach adenocarcinoma.

and AGS GC cells were transfected with siRNAs against ASF1B and scrambled si-NC. First, it was confirmed that HGC-27 and AGS cell models with silenced ASF1B expression were successfully established (Fig. 2A and B). Furthermore, in both HGC-27 and AGS cells, ASF1B expression in the si2-ASF1B group was lower than that in the si1-ASF1B group (Fig. 2A and B). The CCK-8 and colony formation assays indicated that cell proliferation was significantly reduced after ASF1B knockdown (Fig. 2C and D). Additionally, attenuation of ASF1B expression remarkably improved the apoptotic rate of HGC-27 and AGS cells compared with the si-NC group (Fig. 2E).

Knockdown of ASF1B inhibits GC cell migration and invasion. Subsequently, wound healing and Transwell experiments were conducted to explore the effect of ASF1B on the migratory and invasive ability of GC cells. Knockdown of ASF1B inhibited cell migration in both HGC-27 and AGS cells (Fig. 3A). Consistently, the results of Transwell assay verified that the number of invaded cells was decreased after ASF1B knockdown, compared with the si-NC group (Fig. 3B). Furthermore, western blotting revealed that MMP-7 and MMP-9 protein levels were notably attenuated in HGC-27 and AGS cells transfected with si-ASF1B compared with the si-NC group (Fig. 3C).

Knockdown of ASF1B inhibits cisplatin resistance in GC cells. It was hypothesized that ASF1B may affect the sensitivity of GC cells to cisplatin. Due to the difference in sensitivity of different tumor cells to cisplatin (23,24), HGC-27 and AGS cells in the si-NC and si2-ASF1B groups were treated with different doses of cisplatin. CCK-8

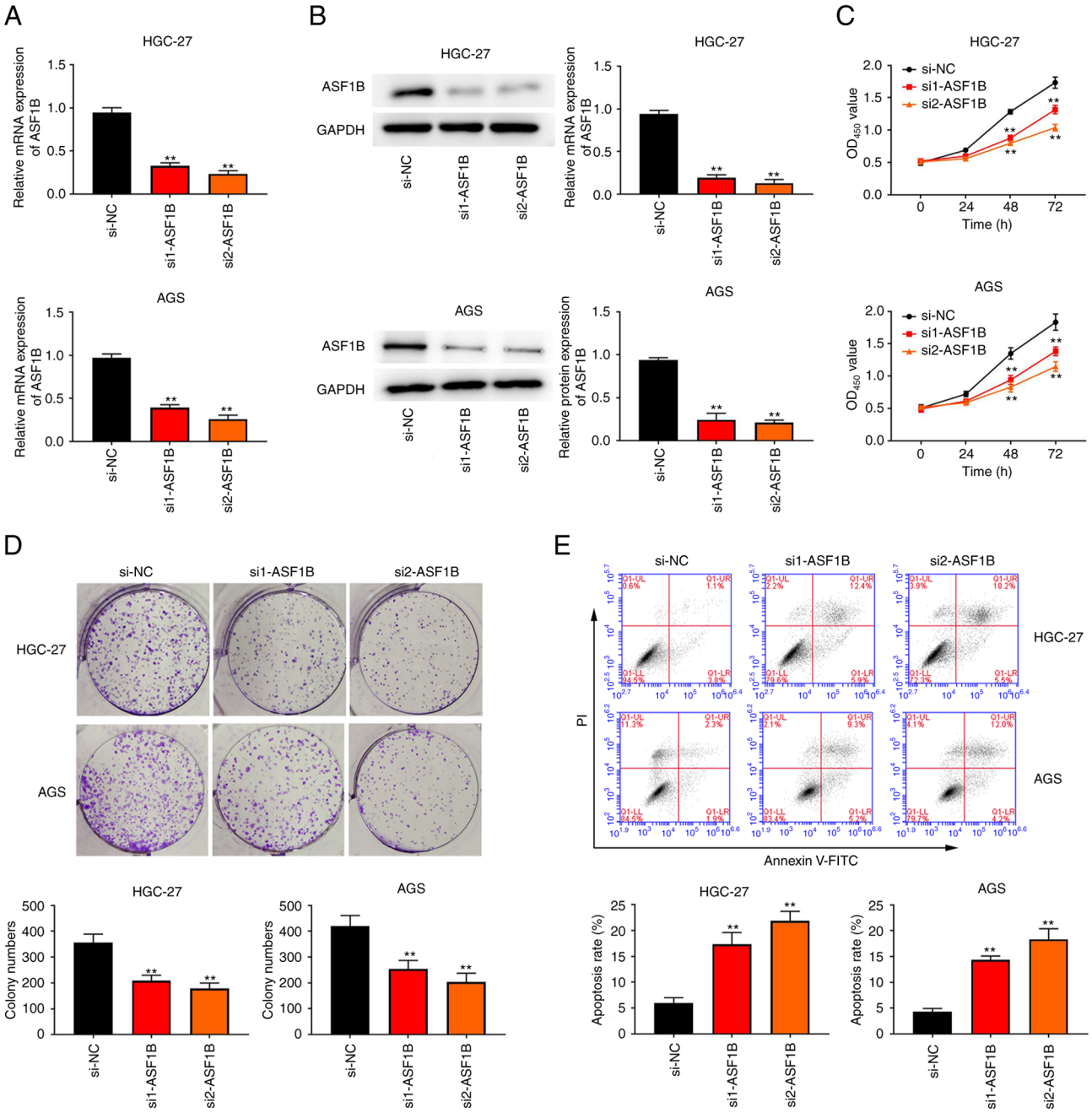

Figure 2. Knockdown of ASF1B inhibits proliferation and induces apoptosis in gastric cancer cells. (A) Reverse transcription-quantitative polymerase chain reaction was performed to analyze the mRNA expression of ASF1B in HGC-27 and AGS cells. (B) ASF1B protein expression was detected by western blotting. (C) Cell Counting Kit-8 assay was conducted to assess the viability of HGC-27 and AGS cells. (D) Proliferation of HGC-27 and AGS cells was evaluated using colony formation assay. (E) Cell apoptosis in HGC-27 and AGS cells was estimated using flow cytometry. **P<0.01 compared with si-NC. ASF1B, anti-silencing function-1B; si, small interfering; NC, negative control.

results showed that the proliferative potential of HGC-27 and AGS cells transfected with si2-ASF1B was lower than that in the si-NC group under cisplatin treatment (Fig. 4A). In both HGC-27 and AGS cells, the IC_{50} for cisplatin was markedly decreased in the si2-ASF1B group compared with the si-NC group (Fig. 4B). As shown in Fig. 4C, the addition of cisplatin increased the inhibitory effect of ASF1B knockdown on colony formation in GC cells. Apoptosis analysis showed that the apoptotic rate of GC cells treated with cisplatin markedly increased compared with the si-NC group, and the combination of si2-ASF1B with cisplatin treatment further enhanced the apoptotic rate of both HGC-27 and AGS cells compared with the si-NC + cisplatin group (Fig. 4D).

Silencing ASF1B attenuates the Myc signaling pathway. To detect the underlying mechanism of ASF1B in GC progression, analysis of expression profiles from TCGA database indicated that the Myc-targets-v1 and Myc-targets-v2 pathways could be activated by ASF1B (Fig. 5A). Subsequently, the interaction of the downstream genes of the Myc-targets-v1 and Myc-targets-v2 pathways was explored and a total of 16

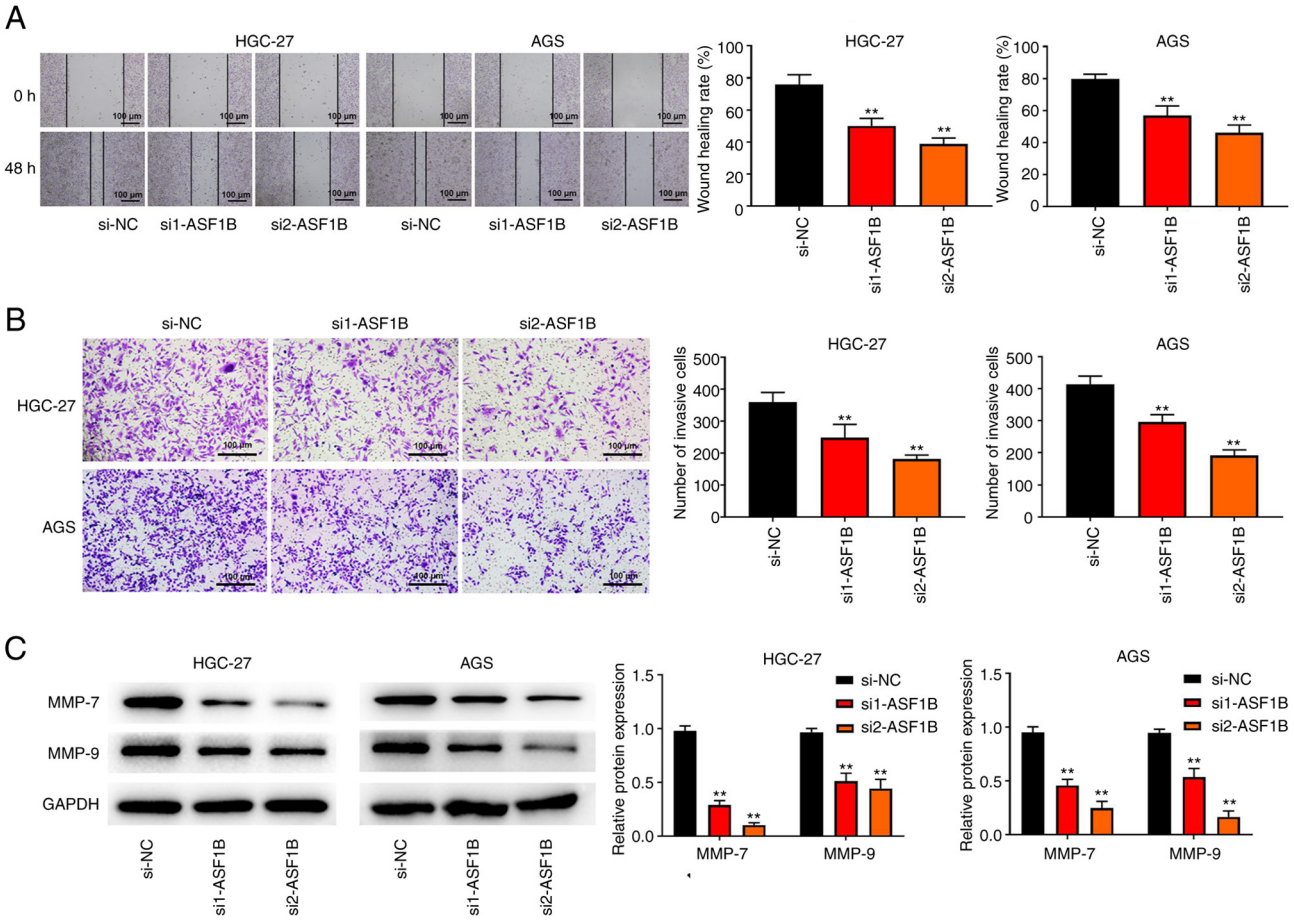

Figure 3. Knockdown of ASF1B inhibits gastric cancer cell migration and invasion. (A) Wound healing assay was employed to assess the migration of HGC-27 and AGS cells. (B) The invasive ability of HGC-27 and AGS cells was determined using Transwell assay. (C) The protein expression levels of MMP-7 and MMP-9 in HGC-27 and AGS cells were examined using western blotting. $^{**}P<0.01$ compared with si-NC. ASF1B, anti-silencing function-1B; si, small interfering; NC, negative control.

overlapping genes were obtained, including Myc, MCM4 and MCM5 (Fig. 5B). Pearson's correlation analysis revealed that Myc, MCM4 and MCM5 expression were positively correlated with the expression of ASF1B (Fig. 5C-E). Following ASF1B knockdown, the protein levels of Myc, MCM4 and MCM5 were all markedly attenuated in HGC-27 and AGS cells (Fig. 5F).

ASF1B regulates cell proliferation, apoptosis, invasion and the cisplatin resistance of GC cells by regulating the Myc pathway. Compared with GES-1 cells, AGS cells showed high ASF1B expression. To further examine the molecular mechanism of ASF1B in GC, AGS cells were selected for Myc overexpression. Successful Myc overexpression is shown in Fig. 6A. Transfection of the Myc overexpression plasmid increased Myc protein expression compared with the si2-ASF1B + Vector group (Fig. 6B). Colony formation experiments revealed that overexpression of Myc reversed the suppressive role of si2-ASF1B on cell proliferation (Fig. 6C). In addition, overexpression of Myc increased the number of invasive cells compared with the si2-ASF1B + Vector group (Fig. 6E). Compared with the si2-ASF1B + Vector group, the si2-ASF1B + Myc group exhibited a higher IC_{50} for cisplatin (Fig. 6F). Furthermore, it was observed that Myc overexpression significantly reversed the promotion of apoptosis caused by ASF1B silencing in AGS cells, both with or without cisplatin treatment (Fig. 6D and G).

Discussion

GC is a prevalent malignancy worldwide, and surgical treatment is considered the fundamental approach to curing this tumor. For patients diagnosed with early GC, survival rates after surgery can reach >90% (25). However, due to the low diagnostic rate of early GC, patients with advanced GC mainly benefit from chemotherapy (26). The effect of chemotherapy on improving survival has been previously reported by data analysis and systematic reviews on individuals with GC (27). Additionally, since GC is an aggressive disease and systemic metastasis is present in most patients with GC (28), chemotherapy has a critical role in GC treatment Nevertheless, drug resistance often leads to an unfavorable prognosis for patients with GC. Therefore, it is urgent to explore novel genes to identify potential therapeutic targets for drug resistance.

The present study revealed that ASF1B was highly expressed in GC tissues and cells. High expression of ASF1B was associated with poor outcomes of patients with GC. These results are similar to those of previous studies. For example, based on a comprehensive pan-cancer analysis, Hu *et al* (29) indicated

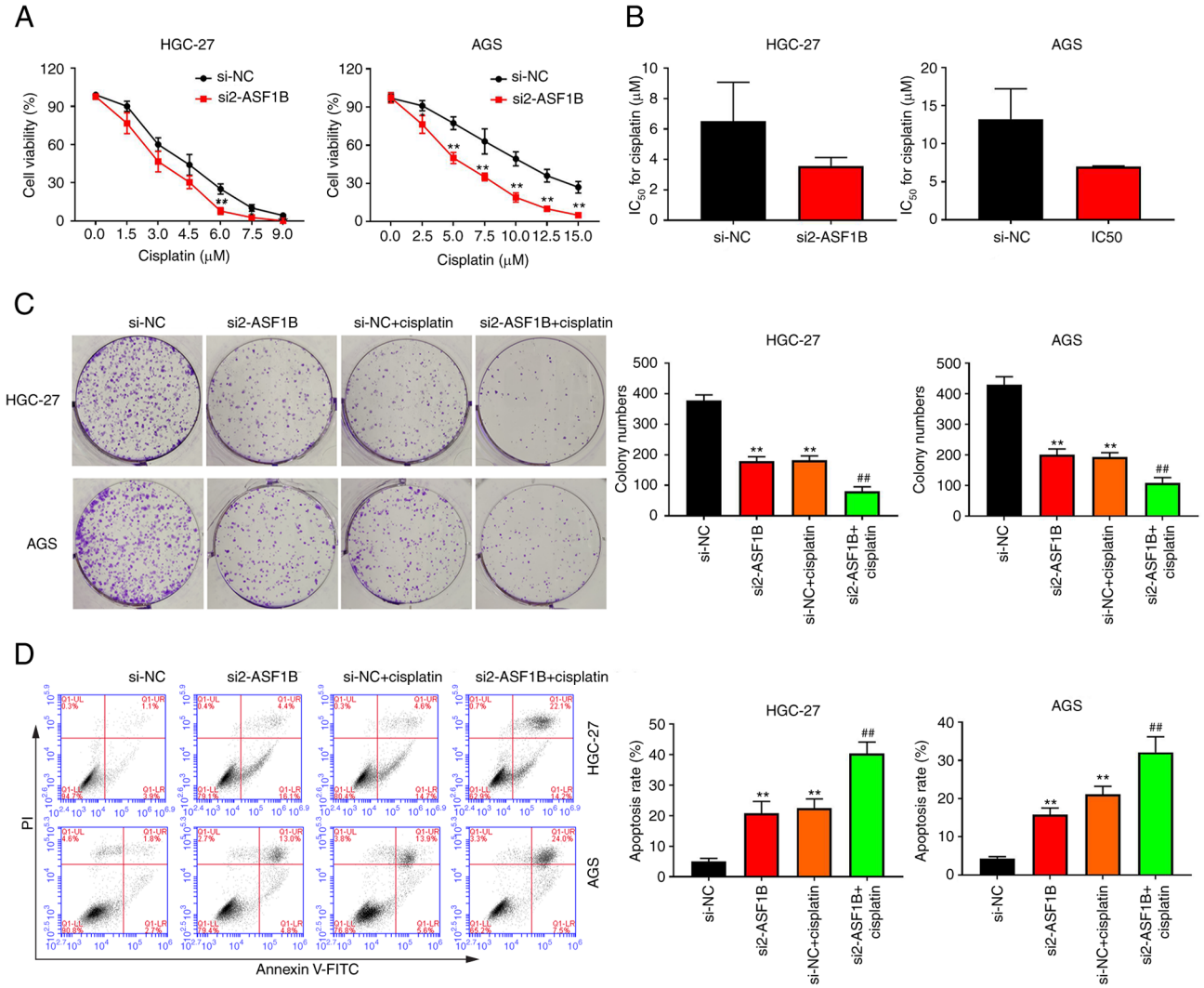

Figure 4. Silencing of ASF1B attenuates the cisplatin resistance of gastric cancer cells. (A) HGC-27 and AGS cells were treated with different concentrations of cisplatin. After 48 h, cell viability was detected using Cell Counting Kit-8 assay. (B) IC_{50} of HGC-27 and AGS cells. (C) Proliferation of HGC-27 and AGS cells was evaluated using colony formation assay. (D) Flow cytometry was used to measure the apoptosis rate of HGC-27 and AGS cells. **P<0.01 compared with si-NC; $^{\#\#}$P<0.05 compared with si-NC + cisplatin. ASF1B, anti-silencing function-1B; si, small interfering; NC, negative control.

that ASF1B was a prognostic and immunological biomarker in nermous cancers, such as adrenocortical cancer, bladder cancer, breast cancer and lung adenocarcinoma. Furthermore, ASF1B has been determined to be a biomarker for the prognosis of thyroid cancer (17), and increased levels of ASF1B in human lung tissues and cells have been associated with poor prognosis and metastasis (30). However, there is no evidence for the effect of ASF1B on GC development, to the best of our knowledge. To detect the functions of ASF1B, *in vitro* experiments were performed. Silencing ASF1B expression suppressed GC cell proliferation, migration and invasion, and induced cell apoptosis. Furthermore, it was demonstrated that cisplatin resistance was significantly reduced following ASF1B knockdown. Cisplatin is known for its strong anticancer activity and is widely used in chemotherapy (31). However, the emergence of cisplatin resistance significantly affects therapeutic outcomes, thereby inducing the tumor recurrence (32,33). In summary, the present results suggested that ASF1B is an important therapeutic target for patients with GC.

Moreover, to explore the underlying mechanism of ASF1B in GC, GSEA was performed. The results suggested that ASF1B was associated with the activation of the Myc-targets-v1 and Myc-targets-v2 signaling pathways. Members of the Myc family are regarded as oncogenes and exert crucial roles in the progression of multiple malignances (34). Myc is an important transcription activator, which can regulate numerous genes and modulate cell viability and apoptosis (35). In addition, the expression of double-stranded DNA break repair genes, such as poly(ADP-Ribose) polymerase 1 and DNA ligase 3, have been indicated to be influenced by Myc (36,37). A number of studies have illustrated that Myc is able to mediate drug resistance in hepatocellular carcinoma, prostate cancer and colorectal cancer (38-40). These findings suggest that Myc may be an alternative therapeutic target for tumor treatment. Therefore, to verify the relationship between ASF1B and the Myc pathway, western blotting was used to measure the protein expression levels of Myc, MCM4 and MCM5

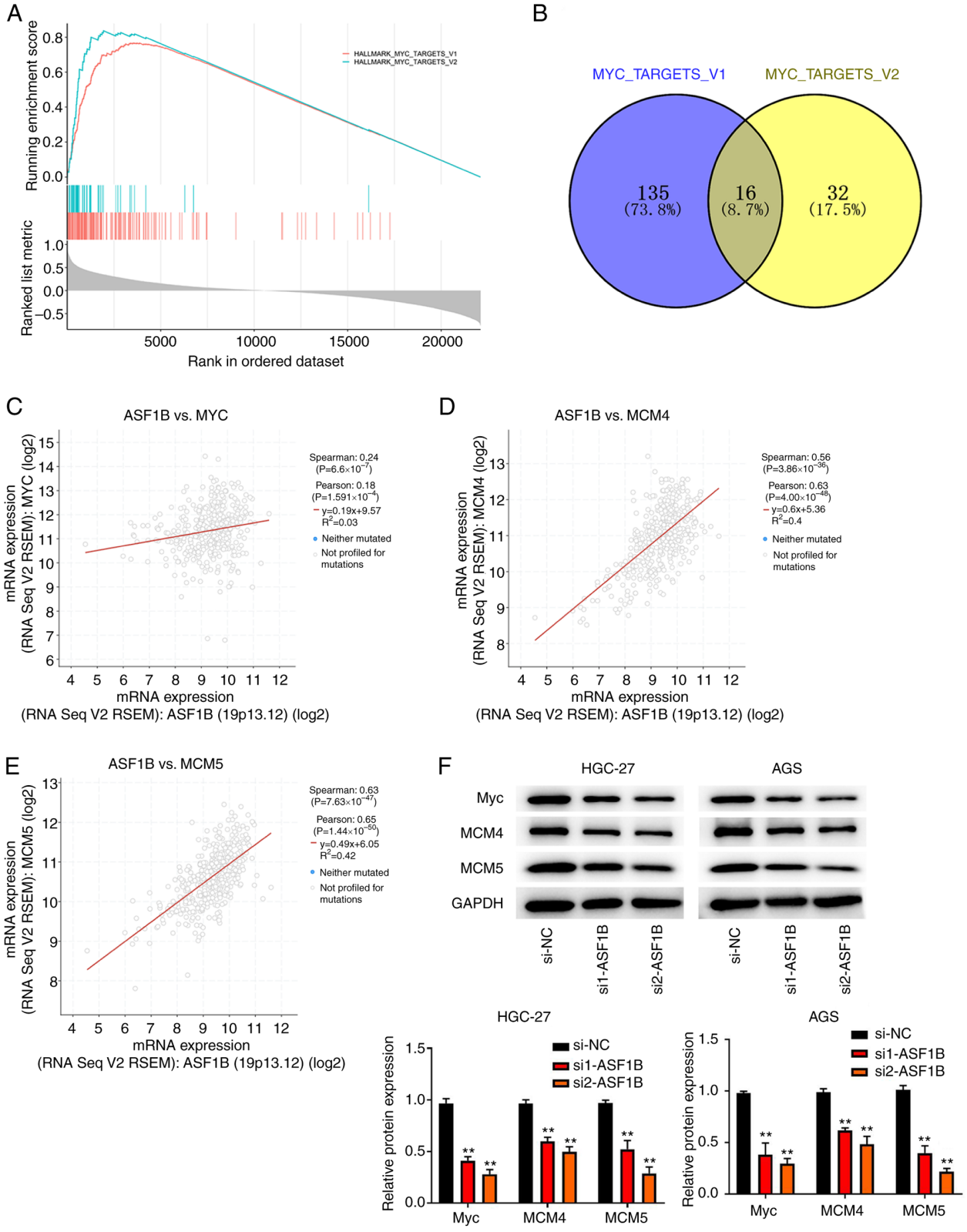

Figure 5. ASF1B silencing attenuates the Myc pathway. (A) Gene set enrichment analysis was used to indicate the relationship between ASF1B and the Myc-targets-v1 and Myc-targets-v2 pathways. (B) Venn diagram highlighting the intersecting genes of the Myc-targets-v1 and Myc-targets-v2 pathways. Myc, MCM4 and MCM5 were selected for subsequent experiments. Pearson's correlation analyses revealed that ASF1B was positively correlated with (C) Myc, (D) MCM4 and (E) MCM5. (F) Protein expression levels of Myc, MCM4 and MCM5 in HGC-27 and AGS cells were semi-quantified using western blotting. **P<0.01 compared with si-NC. ASF1B, anti-silencing function-1B; si, small interfering; NC, negative control.

in HGC-27 and AGS cells after si-ASF1B transfection. The results suggested that reduction of ASF1B expression inhibited the levels of Myc, MCM4 and MCM5. Therefore, it was assumed that ASF1B may regulate the cisplatin resistance of GC through the Myc pathway. The present results revealed that the suppressive effect of ASF1B knockdown

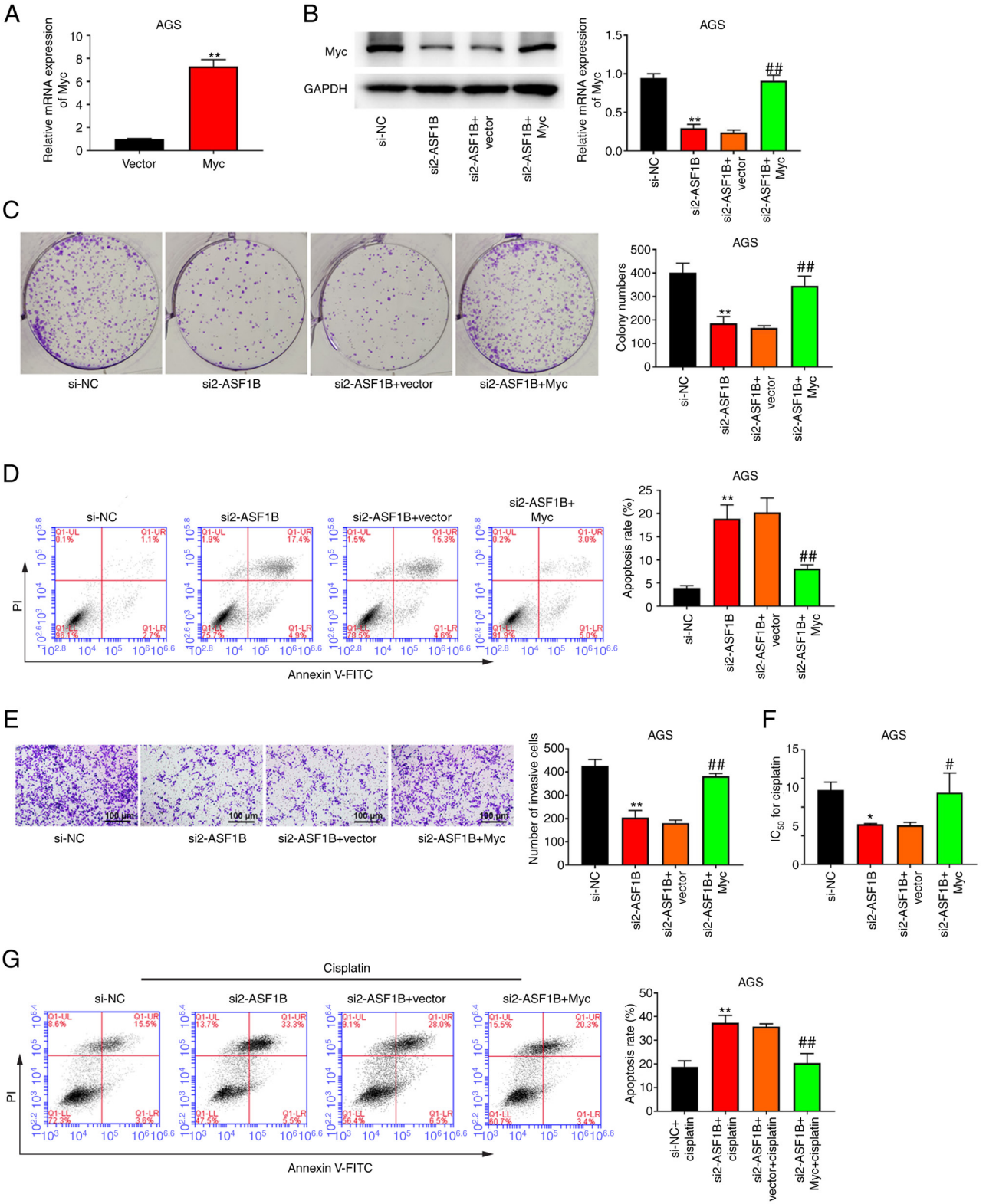

Figure 6. ASF1B regulates cell proliferation, apoptosis, invasion and the cisplatin resistance of gastric cancer cells through the Myc pathway. (A) Reverse transcription-quantitative polymerase chain reaction was used to detect Myc mRNA expression in AGS cells. (B) Myc protein expression was detected by western blotting. (C) Colony formation assay was performed to examine the proliferation of AGS cells. (D) Apoptosis of AGS cells was measured using flow cytometry. (E) Transwell assay was implemented to evaluate the invasive ability of AGS cells. (F) IC_{50} value of AGS cells. (G) Apoptosis of AGS cells was measured using flow cytometry. *P<0.05 and **P<0.01 compared with Vector or si-NC; $^{\#}$P<0.05 and $^{\#\#}$P<0.01 compared with si2-ASF1B + Vector or si2-ASF1B + Vector + cisplatin. ASF1B, anti-silencing function-1B; si, small interfering; NC, negative control.

on cisplatin resistance was reversed by Myc overexpression. Moreover, Myc overexpression reversed the inhibitory effect of ASF1B silencing on GC cell proliferation and invasion.

In conclusion, the present study demonstrated that downregulation of ASF1B may attenuate cell proliferation, invasion and cisplatin resistance by regulating the Myc

pathway, suggesting that ASF1B may be a therapeutic target for cisplatin-based chemotherapy in GC.

Acknowledgements

Not applicable.

Funding

No funding was received.

Availability of data and materials

The datasets used and/or analyzed during the current study are available from the corresponding author on reasonable request.

Authors' contributions

ZZ, MN and JZ designed the research study. ZZ and MN performed the experiments. ZZ and JZ contributed essential reagents or tools. LL, ZL and YW analyzed the data. ZZ and MN confirm the authenticity of all the raw data. ZZ wrote the manuscript. All authors have read and approved the final manuscript.

Ethics approval and consent to participate

All procedures involving human participants were performed in accordance with The Declaration of Helsinki. The research protocol was approved by the Ethics Committee of Cangzhou Central Hospital (Cangzhou, China; approval no. 2021-018-01). Written informed consent was obtained from all patients.

Patient consent for publication

Not applicable.

Competing interests

The authors declare that they have no competing interests.

References

1. Sexton RE, Al Hallak MN, Diab M and Azmi AS: Gastric cancer: A comprehensive review of current and future treatment strategies. Cancer Metastasis Rev 39: 1179-1203, 2020.
2. Brodsky AS, Khurana J, Guo KS, Wu EY, Yang D, Siddique AS, Wong IY, Gamsiz Uzun ED and Resnick MB: Somatic mutations in collagens are associated with a distinct tumor environment and overall survival in gastric cancer. BMC Cancer 22: 139, 2022.
3. Sung H, Ferlay J, Siegel RL, Laversanne M, Soerjomataram I, Jemal A and Bray F: Global Cancer Statistics 2020: GLOBOCAN estimates of incidence and mortality worldwide for 36 cancers in 185 countries. CA Cancer J Clin 71: 209-249, 2021.
4. Tan Z: Recent advances in the surgical treatment of advanced gastric cancer: A Review. Med Sci Monit 25: 3537-3541, 2019.
5. Joshi SS and Badgwell BD: Current treatment and recent progress in gastric cancer. CA Cancer J Clin 71: 264-279, 2021.
6. Kenmotsu H, Yamamoto N, Yamanaka T, Yoshiya K, Takahashi T, Ueno T, Goto K, Daga H, Ikeda N, Sugio K, *et al*: Randomized phase III study of pemetrexed plus cisplatin versus vinorelbine plus cisplatin for completely resected stage II to IIIA nonsquamous non-small-cell lung cancer. J Clin Oncol 38: 2187-2196, 2020.
7. Jiang DM, Gupta S, Kitchlu A, Meraz-Munoz A, North SA, Alimohamed NS, Blais N and Sridhar SS: Defining cisplatin eligibility in patients with muscle-invasive bladder cancer. Nat Rev Urol 18: 104-114, 2021.
8. Hao L, Wang JM, Liu BQ, Yan J, Li C, Jiang JY, Zhao FY, Qiao HY and Wang HQ: m6A-YTHDF1-mediated TRIM29 upregulation facilitates the stem cell-like phenotype of cisplatin-resistant ovarian cancer cells. Biochim Biophys Acta Mol Cell Res 1868: 118878, 2021.
9. Safi A, Bastami M, Delghir S, Ilkhani K, Seif F and Alivand MR: miRNAs modulate the dichotomy of cisplatin resistance or sensitivity in breast cancer: An update of therapeutic implications. Anticancer Agents Med Chem 21: 1069-1081, 2021.
10. Liu L, Fan J, Ai G, Liu J, Luo N, Li C and Cheng Z: Berberine in combination with cisplatin induces necroptosis and apoptosis in ovarian cancer cells. Biol Res 52: 37, 2019.
11. Zhu L, Yuan Y, Yuan L, Li L, Liu F, Liu J, Chen Y, Lu Y and Cheng J: Activation of TFEB-mediated autophagy by trehalose attenuates mitochondrial dysfunction in cisplatin-induced acute kidney injury. Theranostics 10: 5829-5844, 2020.
12. Raudenska M, Balvan J, Fojtu M, Gumulec J and Masarik M: Unexpected therapeutic effects of cisplatin. Metallomics 11: 1182-1199, 2019.
13. Cocetta V, Ragazzi E and Montopoli M: Links between cancer metabolism and cisplatin resistance. Int Rev Cell Mol Biol 354: 107-164, 2020.
14. Ouyang X, Lv L, Zhao Y, Zhang F, Hu Q, Li Z, Zhu D and Li L: ASF1B serves as a potential therapeutic target by influencing cell cycle and proliferation in hepatocellular carcinoma. Front Oncol 11: 801506, 2021.
15. Liu X, Song J, Zhang Y, Wang H, Sun H, Feng X, Hou M, Chen G, Tang Q and Ji M: ASF1B promotes cervical cancer progression through stabilization of CDK9. Cell Death Dis 11: 705, 2020.
16. Wu L and Jie B: Protumor effects of histone H3-H4 chaperone antisilencing Feature 1B gene on lung adenocarcinoma: In silico and in vitro analyses. Comput Math Methods Med 16: 5005459, 2021.
17. Ma J, Han W and Lu K: Comprehensive pan-cancer analysis and the regulatory mechanism of ASF1B, a gene associated with thyroid cancer prognosis in the tumor micro-environment. Front Oncol 11: 711756, 2021.
18. Zhan T, Gao X, Wang G, Li F, Shen J, Lu C, Xu L, Li Y and Zhang J: Construction of novel lncRNA-miRNA-mRNA network associated with recurrence and identification of immune-related potential regulatory axis in hepatocellular carcinoma. Front Oncol 11: 626663, 2021.
19. Jiangqiao Z, Tao Q, Zhongbao C, Xiaoxiong M, Long Z, Jilin Z and Tianyu W: Anti-silencing function 1B histone chaperone promotes cell proliferation and migration via activation of the AKT pathway in clear cell renal cell carcinoma. Biochem Biophys Res Commun 511: 165-172, 2019.
20. Szász AM, Lánczky A, Nagy Á, Förster S, Hark K, Green JE, Boussioutas A, Busuttil R, Szabó A and Győrffy B: Cross-validation of survival associated biomarkers in gastric cancer using transcriptomic data of 1,065 patients. Oncotarget 7: 49322-49333, 2016.
21. Subramanian A, Tamayo P, Mootha VK, Mukherjee S, Ebert BL, Gillette MA, Paulovich A, Pomeroy SL, Golub TR, Lander ES and Mesirov JP: Gene set enrichment analysis: A knowledge-based approach for interpreting genome-wide expression profiles. Proc Natl Acad Sci USA 102: 15545-15550, 2005.
22. Livak KJ and Schmittgen TD: Analysis of relative gene expression data using real-time quantitative PCR and the 2(-Delta Delta C(T)) method. Methods 25: 402-408, 2001.
23. Zhang J, Lv W, Liu Y, Fu W, Chen B, Ma Q, Gao X and Cui X: Knockdown of serum- and glucocorticoid-regulated Kinase 1 enhances cisplatin sensitivity of gastric cancer through suppressing the nuclear factor kappa-b signaling pathway. Balkan Med J 38: 331-340, 2021.
24. Wang G, Wang X and Han M: Loss of DAB2IP contributes to cell proliferation and cisplatin resistance in gastric cancer. Onco Targets Ther 14: 979-988, 2021.
25. Song W, Cui Z, Liu H, Xue L and Ju H: The expression and prognostic value of miR-195-5p in patients with advanced gastric cancer after chemotherapy. J BUON 25: 2332-2340, 2020.
26. Qiao XL, Zhong ZL, Dong Y and Gao F: LncRNA HMGA1P4 promotes cisplatin-resistance in gastric cancer. Eur Rev Med Pharmacol Sci 24: 8830-8836, 2020.

27. Ge L, Hou L, Yang Q, Wu Y, Shi X, Li J and Yang K: A systematic review and network meta-analysis protocol of adjuvant chemotherapy regimens for resected gastric cancer. Medicine (Baltimore) 98: e14478, 2019.
28. Luo Z, Rong Z and Huang C: Surgery strategies for gastric cancer with liver metastasis. Front Oncol 9: 1353, 2019.
29. Hu X, Zhu H, Zhang X, He X and Xu X: Comprehensive analysis of pan-cancer reveals potential of ASF1B as a prognostic and immunological biomarker. Cancer Med 10: 6897-6916, 2021.
30. Wang W, Xiao L, Pan D and Hu L: ASF1B enhances migration and invasion of lung cancers cell via regulating the P53-mediated epithelial-mesenchymal transformation (EMT) signaling pathway. Neoplasma 69: 369, 2022.
31. Qi L, Luo Q and Zhang Y: Advances in toxicological research of the anticancer drug cisplatin. Chem Res Toxicol 32: 1469-1486, 2019.
32. Li X, Wu X, Yang H, Li L, Ye Z and Rao Y: A nuclear targeted Dox-aptamer loaded liposome delivery platform for the circumvention of drug resistance in breast cancer. Biomed Pharmacother 117: 12, 2019.
33. Liang W, Zheng Y, Zhang J and Sun X: Multiscale modeling reveals angiogenesis-induced drug resistance in brain tumors and predicts a synergistic drug combination targeting EGFR and VEGFR pathways. BMC Bioinformatics 20 (Suppl 7): S203, 2019.
34. Li Y, Zu X, Hu X, Wang L and He W: Forkhead Box R2 knockdown decreases chemoresistance to cisplatin via MYC pathway in bladder cancer. Med Sci Monit 25: 8928-8939, 2019.
35. Mei Y, Liu YB, Hu DL and Zhou HH: Effect of RIF1 on response of non-small-cell lung cancer patients to platinum-based chemotherapy by regulating MYC signaling pathway. Int J Biol Sci 14: 1859-1872, 2018.
36. Pyndiah S, Tanida S, Ahmed KM, Cassimere EK, Choe C and Sakamuro D: c-MYC suppresses BIN1 to release poly(ADP-ribose) polymerase 1: A mechanism by which cancer cells acquire cisplatin resistance. Sci Signal 4: 2001556, 2011.
37. Muvarak N, Kelley S, Robert C, Baer MR, Perrotti D, Gambacorti-Passerini C, Civin C, Scheibner K and Rassool FV: c-MYC Generates repair errors via increased transcription of alternative-NHEJ factors, LIG3 and PARP1, in tyrosine kinase-activated leukemias. Mol Cancer Res 13: 699-712, 2015.
38. Xia P, Zhang H, Xu K, Jiang X, Gao M, Wang G, Liu Y, Yao Y, Chen X, Ma W, *et al*: MYC-targeted WDR4 promotes proliferation, metastasis, and sorafenib resistance by inducing CCNB1 translation in hepatocellular carcinoma. Cell Death Dis 12: 691, 2021.
39. Li M, Fang L, Kwantwi LB, He G, Luo W, Yang L, Huang Y, Yin S, Cai Y, Ma W, *et al*: N-Myc promotes angiogenesis and therapeutic resistance of prostate cancer by TEM8. Med Oncol 38: 127, 2021.
40. Sun W, Li J, Zhou L, Han J, Liu R, Zhang H, Ning T, Gao Z, Liu B, Chen X and Ba Y: The c-Myc/miR-27b-3p/ATG10 regulatory axis regulates chemoresistance in colorectal cancer. Theranostics 10: 1981-1996, 2020.